BASE ANGULAR LAYOUT OPTIMIZATION OF THE HEXA PARALLEL ROBOT BASED ON A SINGULARITY INDEX

Alexandre Campos alexandre.campos@joinville.udesc.br
Pablo Muñoz-Rojas pablo@joinville.udesc.br
Marcelo da Silva Hounsell marcelo@joinville.udesc.br
Universidade do Estado de Santa Catarina - Campus Universitário - Joinville - SC - Brazil

Marco Luersen luersen@utfpr.edu.br
Universidade Tecnológica Federal do Paraná - Av. Sete de Setembro, 3165 - Curitiba - PR - Brazil

Abstract. *In the last decades, parallel robots have been intensively studied and employed as an alternative to serial manipulators. The reason is related to well-known enhanced characteristics, such as accuracy, rigidity and high load-to-weight ratio. However, parallel configurations are prone to present direct kinematic singularities, which might cause important constraints in their allowable inner workspace. Previous works, set in the frame of screw theory to represent robot movements and actions, report the existence of an index which indicates the entrance of an Hexa parallel robot to all its direct kinematic singularities. This paper presents an optimization procedure to maximize the robot workspace based on the aforementioned singularity index. The proposed strategy consists of two nested loops. In the inner loop the path imposed to the effector is divided into finite increments for given geometrical parameters of the robot. At the end of each increment, an optimization problem is solved, in which the power inspired measure is adopted as an objective function to be minimized. The corresponding design variables in the inner optimization are related to the orientation of the axis which presents minimal resistance to a unit spin. Thus, at each considered point along the effector path, the singularity index is obtained. In the outer loop, the end-effector maximal rotation angle limited by the singularity indexes obtained in the inner loop is adopted as objective function (to be maximized). In this loop, the angle among robot legs, i.e. the base angular layout, are employed as design variables. The procedure is implemented in the frame of MATLAB platform and uses built- in mathematical programming routines for constrained optimization. The use of mathematical programming tools gives wide generality for treating complex design problems and this study is a first step towards more complex situations.*

Keywords: *Parallel Robot, Dimensional Synthesis, Direct Singularity, Power Inspired Index)*

1. INTRODUCTION

A closed kinematic chain mechanism where a special link, *i.e.* end-effector, is linked to the fixed base by several independent kinematic chains is named a parallel robot (Merlet, 2000). Therefore parallel robots consist of a set of parallel legs each with active and passive joints required to maintain the system mobility and controllability. Parallel legs connect the base to the moving platform resulting in structures able to achieve high stiffness and high force-to-weight ratio. However, parallel robots, such as the Hexa robot in Fig. 1 (Hesselbach et al., 2005), are known for low dexterity and a restricted workspace, limited by direct and inverse kinematic singularities (Campos et al., 2008). Thence, it is convenient to enlarge the robot workspace regarding its stiffness.

Direct singularities allow the end effector to gain unconstrained movements without any actuated joint movement. This kind of singularity drives the robot to uncontrollable movements that may produce permanent damage to the robot's structure and surrounding equipment (Wolf and Shoham, 2003).

Direct singularities identification has been studied from different perspectives: vanishing of the Jacobian determinant (Mohammadi-Daniali et al., 1995), qualitative conditions, based on line geometry (Merlet, 2000), linear decomposition and cofactor expansion of the determinant for general Gough-Stewart platform in a given orientation (Mayer and Gosselin, 2000) and some numerical approaches like condition number (Xu et al., 1994), natural frequency measure (Voglewede and Ebert-Uphoff, 2004) and the power and the stiffness inspired measure (Pottmann et al., 1998a; Wolf and Shoham, 2003; Campos et al., 2009).

The purpose of optimization is to aim at enhancing the performance indexes, *e.g.* the workspace, by adjusting parameters, such as the link length, the radii of fixed and moving platforms etc. This approach is called the dimensional synthesis-based performance optimization of parallel manipulators (Gao et al., 2010).

Many researchers have faced the optimum design problem for robot manipulators (Zhang et al., 2006; Rout, 2008; Yu et al., 2008). Zhao et al. (2007) used the least number method for variables in order to optimize the parallel manipulator leg length aiming at dexterous workspace. A method for the multi-dimensional kinematic optimization of the geometry for the linear delta robot architecture is presented by Stock and Miller (2003). Additionally, Ceccarelli and Lanni (2004) studied a multi-objective optimization problem for a 3R manipulator with prescribed workspace limits using an algebraic formulation. It is important to notice that artificial intelligence techniques can be widely applied to this research topic.

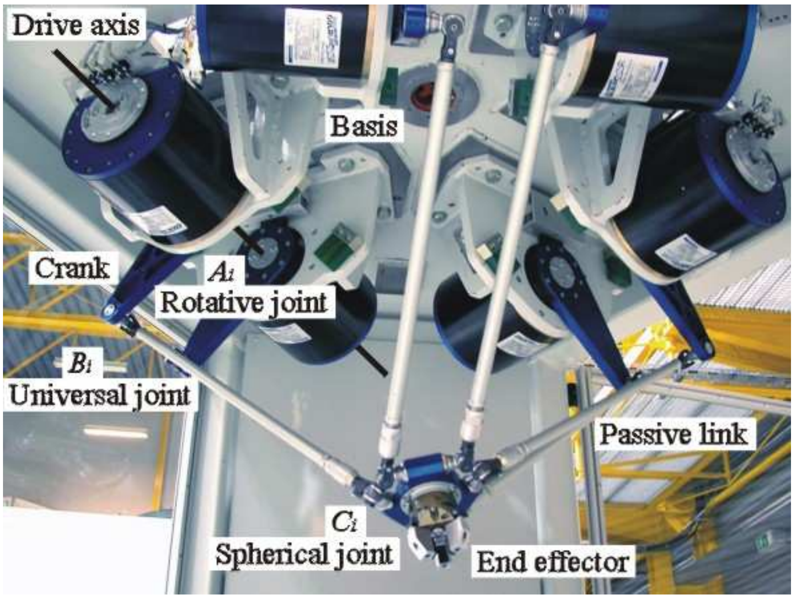

Figure 1. Hexa parallel robot of the Collaborative Research Center 562

In this paper, initially instantaneous movements and actions are presented by screws and velocity or action magnitudes, respectively, *i.e.* twists or wrenches. Parallel manipulator singularities and some methods to detect them are also introduced shortly. Then the optimization procedure and its application to the Hexa parallel robot is presented. Finally, the specific geometrical parameters for the Hexa robot aiming at maximum rotation about a given axis considering safe singularity region are obtained.

2. PARALLEL ROBOT MODELING

In order to simulate the singular behavior of parallel robots, the screw theory is used aiming at kinematic and static modeling. The screw is a geometric element composed by a directed line (axis) and by a scalar length parameter h called pitch (Ball, 1900). If the directed line is represented by a normalized vector, the screw is called a normalized screw $\hat{\$}$.

2.1 DIFFERENTIAL KINEMATICS

The Mozzi theorem (Ceccarelli, 2000) states that the velocities of points on a rigid body with respect to an inertial reference frame $O(X, Y, Z)$ may be represented by a differential rotation $\boldsymbol{\omega}$ about a given fixed axis and a simultaneous differential translation $\boldsymbol{\kappa}$ along the same axis. The complete movement of the rigid body, combining rotation and translation, is called screw movement or twist \$. The body "twists" around an axis instantaneously fixed with respect to the inertial reference frame. This axis is called the screw axis and the rate of the translational velocity and the angular velocity is called the pitch of the screw $h = \|\boldsymbol{\kappa}\|/\|\boldsymbol{\omega}\|$.

The twist represents the differential movement of the body with respect to the inertial frame and may be expressed by a pair of vectors, in ray order, as (Hunt, 2000)

$$\$ = \begin{bmatrix} \boldsymbol{\omega} \\ \boldsymbol{V_p} \end{bmatrix} = \begin{bmatrix} \mathcal{L} \, \mathcal{M} \, \mathcal{N} \, \mathcal{P}^* \, \mathcal{Q}^* \, \mathcal{R}^* \end{bmatrix}^T . \tag{1}$$

Here ω is the angular velocity of the body with respect to the inertial frame and $\boldsymbol{V_p}$ represents the linear velocity of a point P attached to the body, which is instantaneously coincident with frame O. It is possible to express the same twist in axis order $\$ = [\mathcal{P}^* \, \mathcal{Q}^* \, \mathcal{R}^* \, \mathcal{L} \, \mathcal{M} \, \mathcal{N}]^T$.

The vector $\boldsymbol{V_p}$ consists of two components: a) a velocity component parallel to the screw axis represented by $\tau = h\boldsymbol{\omega}$; and b) a velocity component normal to the screw axis represented by $\boldsymbol{S_o} \times \boldsymbol{\omega}$, where $\boldsymbol{S_o}$ is the position vector of any point at the screw axis.

A twist may be decomposed into its magnitude Ψ and its corresponding normalized screw $\hat{\$}$, *i.e.* $\$ = \hat{\$}\Psi$ (Hunt, 2000).

2.2 STATICS

In the same way, the Poinsot theorem (Poinsot, 1806; Hunt, 1978) states that a general action, *i.e.* a force and a couple, upon a rigid body may be carried by a screw, called wrench $\$'$ (Ball, 1900; Hunt, 2000). In this case the wrench in ray

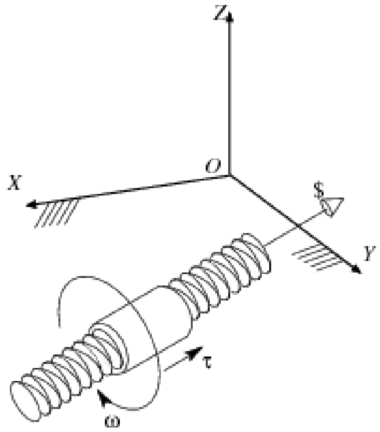

Figure 2. Twist components for a general screw kinematic pair

order is

$$\$' = \begin{bmatrix} \boldsymbol{f} \\ \boldsymbol{C_O} \end{bmatrix} = \begin{bmatrix} \mathcal{L}' \ \mathcal{M}' \ \mathcal{N}' \ \mathcal{P}^{*\prime} \ \mathcal{Q}^{*\prime} \ \mathcal{R}^{*\prime} \end{bmatrix}^T \tag{2}$$

where $\boldsymbol{f}$ is the resultant force and $\boldsymbol{C_O}$ is the resultant couple around O, upon the body. The wrench may be decomposed as $\$' = \hat{\$}'\tau$ where τ is the wrench magnitude and the $\hat{\$}' = [L' \ M' \ N' \ P^{*\prime} \ Q^{*\prime} \ R^{*\prime}]$ is the normalized screw. The wrench pitch is determinated by $h' = \|C_\|\|/\|f\|$, being $C_\|$ the couple component in the screw axis direction.

2.3 POWER

Consider a rigid body supporting a wrench ($\$' = \left[\boldsymbol{f}^T \boldsymbol{C_O}^T\right]^T$) while it is moving around an instantaneous twist ($\$ = \left[\boldsymbol{\omega}^T \boldsymbol{V_p}^T\right]^T$). Therefore, the power carried out is (Ball, 1900; Hunt, 2000)

$$\delta W = \boldsymbol{C_O} \cdot \boldsymbol{\omega} + \boldsymbol{f} \cdot \boldsymbol{V_p} = \$'^T \$ \tag{3}$$

where $\$'$ and $\$$ are given in axis and ray order, respectively.

The screw theory is suitable to represent parallel manipulator end effector movements and actions which are used to detect singularities.

2.4 PARALLEL ROBOT SINGULARITY DETECTION

In this section a differential kinematic relation for parallel manipulators and the singular behavior is presented, and the method used to detect their direct singularities is introduced.

2.4.1 Robot Singularity

In spatial parallel manipulators, the relationship between actuator coordinates q and end effector Cartesian coordinates x, may be stated as a function f

$$f(\boldsymbol{q}, \boldsymbol{x}) = \boldsymbol{0} \tag{4}$$

where $\boldsymbol{0}$ is the 6-dimensional null vector. Therefore, the differential kinematic relation may be determined as

$$\boldsymbol{J_q \dot{q} - J_x \$ = 0; \dot{q} = J \$} \tag{5}$$

where $\$$ is the end effector velocity twist in ray order and $\boldsymbol{J} = \boldsymbol{J_q}^{-1}\boldsymbol{J_x}$ is the Jacobian of the manipulator composed by direct $\boldsymbol{J_x}$ and inverse $\boldsymbol{J_q}$ Jacobian matrices. Additionally, may be written (5) as a differential kinematic relationship between the end effector velocity $\$$ and the vector $\boldsymbol{v} = [v_1, \cdots, v_n]^T$

$$\boldsymbol{v} = \boldsymbol{J_x}\$ \tag{6}$$

where $\boldsymbol{v}$ is the component of the absolute linear velocity of the end effector connection point (C_i) in the direction of the passive link $\left(\overline{B_iC_i}\right)$ (Davidson and Hunt, 2004), see Fig. 1.

It is important to notice that the rows of the direct kinematic matrix J_x may correspond to the normalized screw of wrenches, in axis order acting upon the end effector through the passive link, *i.e.* the distal link of each limb (serial chain between basis and end effector) (Davidson and Hunt, 2004). Therefore, a static relation may be stated as

$$\boldsymbol{J_x}^T \boldsymbol{\tau} = \left[\hat{\$}_{r1}, \cdots, \hat{\$}_{r6}\right] \boldsymbol{\tau} = \$' \tag{7}$$

where $\$'$ is the resultant wrench acting upon the end effector, in axis order, $\boldsymbol{\tau} = [\tau_1, \cdots, \tau_6]$ are the input wrench magnitudes and the columns of $\boldsymbol{J_x}^T$ are the normalized screws (axial order) of wrenches acting on the end effector.

Singular configurations appear if either $\boldsymbol{J_x}$ or $\boldsymbol{J_q}$ drop rank. If $\boldsymbol{J_q}$ drops rank, *i.e.* it becomes singular, an inverse kinematics singularity is encountered and the end effector is over-constrained (Tsai, 1999), *i.e.* it looses at least one DOF.

The inverse kinematic singularity is found at the boundary of the workspace or when a limb folds upon itself. This type of singularity is caused due to the serial nature of the limbs and is discussed in the literature (Tsai, 1999; Sciavicco and Siciliano, 1996).

If $\boldsymbol{J_x}$ is singular, a direct singularity is encountered and the end effector can even move if all actuators are locked. At these configurations, the end effector gains one or more even uncontrollable degrees of freedom. This type of singularity occurs in the workspace and is the main goal of this paper.

There are three basic reasons why singularities become an issue in real life situations: reduced accuracy, large internal forces and loss of knowledge of solution tree, *i.e.* mechanically the manipulator is not where the control believes it is (Voglewede, 2004), and the robot structure may be damaged.

2.4.2 Power Inspired Measure

This technique is developed using the screw theory, specifically the power or rate of work, to determine how close the parallel manipulator is to a direct singularity (Pottmann et al., 1998b). The power inspired measure determines closeness to singularity through an optimization problem that results in a corresponding generalized eigenvalue problem. Using this methodology it is possible to describe the instantaneous behavior of the end effector near singularities (Wolf and Shoham, 2003). Other measures are incorporated into a constrained optimization framework, *e.g.* the natural frequency measure (Voglewede, 2004).

In this approach the objective function $F(\hat{\$}, \$'_{i=1,\cdots,n})$ to be optimized can be interpreted as the sum of the square of the power (3) of each leg upon the end effector which is constrained to move on $\$(\|\boldsymbol{\omega}\| = 1, h \neq \infty)$, a normalized finite pitch twist; this interpretation may be done assuming unitary magnitude wrenches as normalized screws $\hat{\$}'_i \simeq \$'_i$

$$F = \sum_{i=1}^{n} \left(\hat{\$}_i'^T \$\right)^2 \tag{8}$$

with

$$\hat{\$}'_i = \left[P_i^{*\prime} Q_i^{*\prime} R_i^{*\prime} L'_i M'_i N'_i\right]^T ; \$ = [\mathcal{L}\mathcal{M}\mathcal{N}\mathcal{P}^*\mathcal{Q}^*\mathcal{R}^*]^T \tag{9}$$

where $\hat{\$}'_i$ (dependent on $\boldsymbol{x}$ position coordinates, specifically of C_i and B_i positions) and $\$$ are given in axis and ray order, respectively, and n is the number of limbs.

Therefore, F may be expressed as

$$F = \$^T J_x^T J_x \$ = \$^T \boldsymbol{M} \$; \boldsymbol{M} = \sum_{i=1}^{n} \$'_i \$_i'^T \tag{10}$$

where $\boldsymbol{M}$ is called the Graminiam matrix, and from (6) may be rewritten as

$$F = (\boldsymbol{J_x}\$)^T (\boldsymbol{J_x}\$) = \boldsymbol{v}^T \boldsymbol{v} = \|\boldsymbol{v}\|^2 \tag{11}$$

being $\|\boldsymbol{v}\|$ the Euclidean norm of the vector of linear velocities $\boldsymbol{v}$ (6).

Considering that the only unconstrained movements of the end effector, in a direct singularity, are finite pitch twists (no pure translational movements are permitted) with magnitude $\Psi = 1$, the unitary twist magnitude, which is the constraint of the optimization method, is given through the invariant normalization (Voglewede and Ebert-Uphoff, 2004)

$$\|\$\| = \sqrt{\boldsymbol{\omega} \cdot \boldsymbol{\omega}} = \sqrt{\mathcal{L}^2 + \mathcal{M}^2 + \mathcal{N}^2} = 1 \Rightarrow \|\$\|^2 = \$^T \boldsymbol{D} \$ = 1 \tag{12}$$

where $\boldsymbol{D} = diag\{1, 1, 1, 0, 0, 0\}$.

Equation (10) under the constraint (12) may be transformed to obtain the Lagrangian L,

$$\boldsymbol{L} = \$^T \boldsymbol{M} \$ - \boldsymbol{\lambda}(\$^T \boldsymbol{D} \$ - 1) \tag{13}$$

where λ is the Lagrangian multiplier. The minimization of the Lagrangian is performed by

$$\frac{\partial L}{\partial \boldsymbol{\lambda}} = \$^T \boldsymbol{D}\$ = 1 \; ; \; \frac{\partial L}{\partial \$} = (\boldsymbol{M} - \lambda \boldsymbol{D})\$ = 0. \tag{14}$$

The matrix expression in the parenthesis, for a nontrivial solution, has to be singular, *i.e.*

$$det(\boldsymbol{M} - \boldsymbol{\lambda D}) = 0. \tag{15}$$

Since the objective function is non-negative, given that M is a square symmetric positive semi-definite matrix (Voglewede, 2004), the end effector normalized twist which minimizes the supply power through the wrenches is the eigenvector $\$_{min}$ associated to the smallest eigenvalue λ_{min}. In this case one gets the minimum of F upon the end effector moving on $\$_{min}$, see (12), as

$$\begin{aligned} F(\$_{min}, \hat{\$}'_{i=1,\cdots,6}) &= \$^T_{min} \boldsymbol{M} \$_{min} \\ &= \lambda_{min} \$^T_{min} \boldsymbol{D} \$_{min} = \lambda_{min}. \end{aligned} \tag{16}$$

In direct singularity there is a twist $\$_{min}$ for which none of the limb wrenches can do any work and then the minimum of F, *i.e.* λ_{min}, goes to zero. Out of a singularity, $\$_{min}$ represents the less constrained twist and λ_{min} is a power based function measure that indicates the manipulator singularity closeness. It is worth remarking that $\delta W_{min} = \sqrt{\lambda_{min}}$ represents the minimal power.

The case of two or three similar or identical minimum eigenvalues means that wrenches are in the intersection of two or three linear complexes, *i.e.* a linear congruence or a regulus respectively, and the end effector gains two or three degrees of freedom.

Next, the optimization design procedure is introduced and its application to the Hexa parallel robot is presented.

3. DESIGN OPTIMIZATION

The core of the strategy presented herein is based on two nested optimization loops. The inner loop is given by Eq. (16) and the approach adopted in the outer loop makes use of numerical optimization and employs the so-called interior point algorithm (Haftka and Gürdal, 1991; Rao, 1978; Vanderplaats, 1984). Interior point algorithms belong to the family of first-order gradient based optimization methods, which in a sense, compete with evolutionary or zero-order optimization procedures. Gradient methods typically are able to lead with a large number of design variables and can lead to a minimum (or maximum) within an acceptable computer time. On the other hand, they can easily get trapped in local minima (unless the optimization problem is convex) and many times evaluation of analytical derivatives is cumbersome or even impossible. Combinatorial or evolutionary methods do not pose difficulties concerning derivative calculations (they are not needed), but have severe restrictions for a large number of design variables. Recent research related to the present contribution has employed genetic algorithms and neural networks (Gao et al., 2010) aiming at optimizing the base motor angular layout. However, in our paper, a gradient based approach is proposed due to its rapid performance and to the possibility to increase the number of design variables allowing the future treatment of fairly more complex problems.

Interior point or barrier methods of optimization have the convenient feature that they keep the design in the feasible domain. Although other alternatives exist, typically the interior point method replaces the inequality constrained problem

$$minimize \quad g_0(\mathbf{x})$$

$$s.t. \quad g_j(\mathbf{x}) \leq 0, \quad j = 1, \ldots, n_g$$

by the unconstrained problem

$$minimize \quad \phi(\mathbf{x}, r) = g_0(\mathbf{x}) - r\Sigma_{j=1}^{n_g} ln(g_j)$$

where g_0 is the outer objective function, g_j and s_j are the corresponding inequality constraints and slack variables respectively, n_g is the total number of these constraints, r is a penalty parameter and ϕ is the penalized objective function.

It is noteworthy that due to ill-conditioning, one must solve the optimization problem several times with decreasing r values. Only when r and g_j are small enough simultaneously, the optimum point is found.

The vector $\mathbf{x}$ contains the design variables and ϕ can be either explicitly or implicitly dependent on $\mathbf{x}$. It is assumed that ϕ is twice continuously differentiable with respect to $\mathbf{x}$. Since the penalty term in ϕ is proportional to $ln(s_j)$, the function becomes infinite at the boundary of the feasible domain, imposing a barrier which prevents the design from leaving the feasible area.

Due to numerical reasons, it is sometimes advantageous to use an extended interior penalty method, which combines exterior and interior penalty functions, but will not be described here. The interested reader is referred to Vanderplaats (Vanderplaats, 1984), for instance.

Since there is a small number of design variables, the use of first-order derivative methods of unconstrained optimization is recommended. Among such, some possibilities are steepest descent, conjugate gradients and quasi-newton methods. In this work, MATLAB's function "fmincon" is employed with the following options:

```
 optimset('Algorithm','interior-point','Display','iter','GradObj','on','GradConstr','on',
'TolFun',1e-6,'TolCon',1e-6,'AlwaysHonorConstraints','none','Display','final','PlotFcns'
,{@optimplotx ,@optimplotfval, @optimplotconstrviolation,@optimplotfirstorderopt},
'InitBarrierParam',0.05);
```

where the algorithmic parameters adopted are specified. The necessary gradients are evaluated via user-supplied central finite differences.

4. SOLUTION BASED ON THE POWER INSPIRED INDEX

A typical plot of the singularity index δW_{min} versus the angular position θ through the prescribed path is shown in Fig. 3.

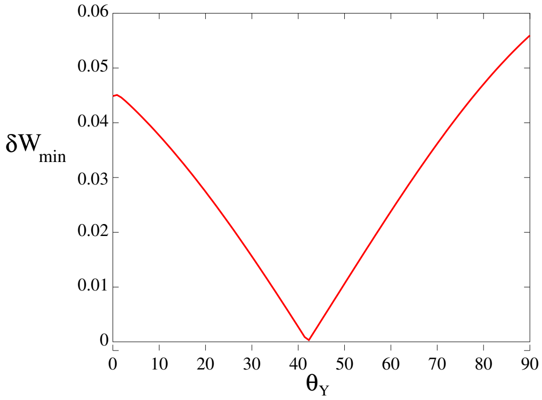

Figure 3. Singularity index versus rotation around Y axis

The curve follows a "V" pattern at whose bottom valley the singularity index approaches zero. It would be of interest to maximize the distance $D(\mathbf{x})$ between the vertical axis and the lower point of the "V" shape, thus yielding a larger working area. In this process, it must be ensured that the initial vertical position of the "V" curve is higher than a singularity limit.

Note that the bottom vertex of the "V" curve does not necessarily intersect the horizontal axis. Hence, an extrapolation procedure is devised in order to compute the objective function with sufficient generality, as displayed in Fig. 4.

The parameters allowed to be modified (design variables) are $\mathbf{x} = [\alpha_1, \alpha_2]$ (see Fig. 5) which are the angles between the pairs of legs, so that the following optimization problem is defined in the outer loop:

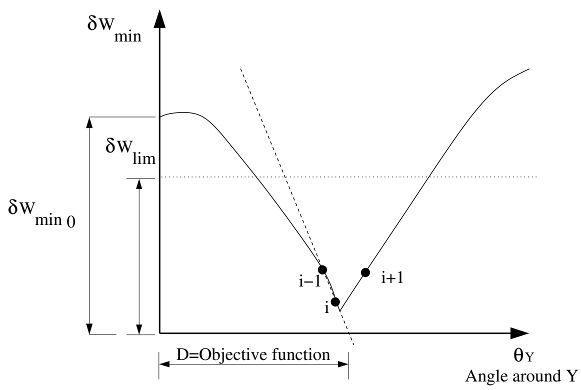

Figure 4. Extrapolation procedure for evaluation of the objective function

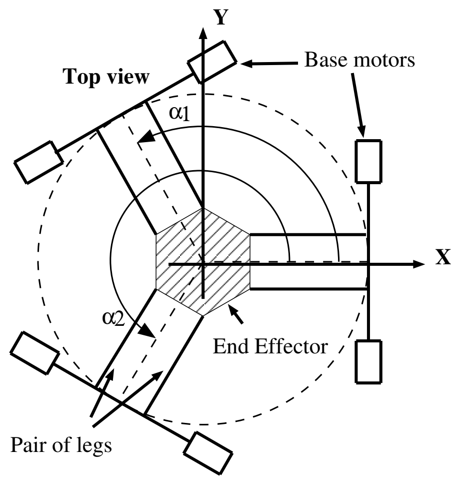

Figure 5. Base angular layout where design parameters are α_1 and α_2

$$
\begin{aligned}
minimize \quad & g_0(\mathbf{x}) = -D(\mathbf{x}) \\
s.t. \quad & g_1(\mathbf{x}) = \delta W_{lim} - \delta W_{min\ 0} \leq 0 \\
& g_2(\mathbf{x}) = \alpha_1 + \epsilon_1 - \alpha_2 \leq 0 \\
& g_3(\mathbf{x}) = -\alpha_1 + \epsilon_2 \leq 0
\end{aligned}
$$

$$g_4(\mathbf{x}) = \alpha_2 - \epsilon_3 \leq 0$$

which is solved by an interior point approach using *fmincon* function available in MATLAB, considering that ϵ_i are constructive constants, and δW_{lim} and $\delta W_{min\ 0}$ are the limit singularity index which constrains the end effector rotation into a safe zone and its initial value, respectively. Note that minimizing $g_0(\mathbf{x}) = -D(\mathbf{x})$ is equivalent to maximize D. The whole optimization approach, *i.e.* inner and outer loop, is depicted in the optimization flow chart shown in Fig. 6.

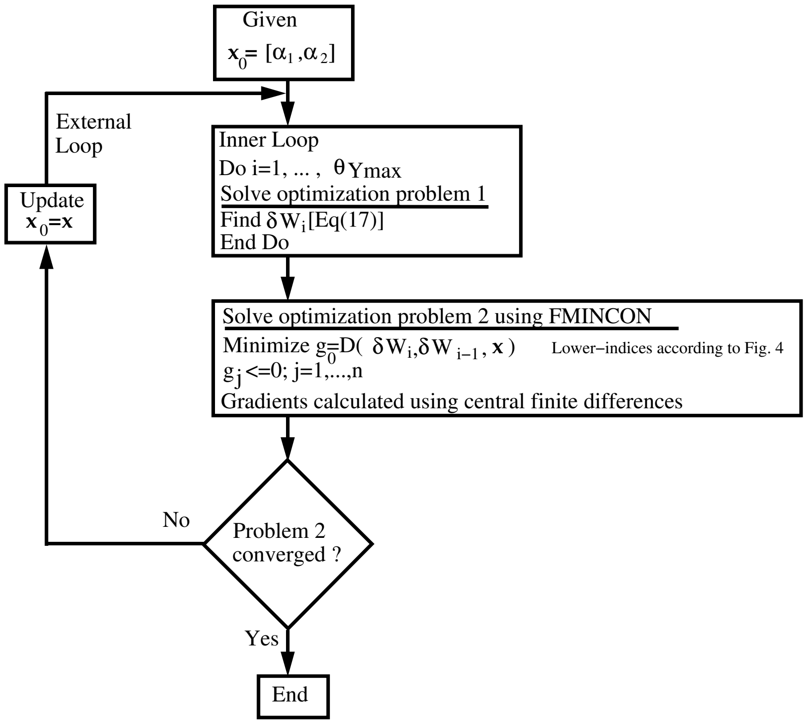

Figure 6. Optimization flow chart

5. APPLICATION TO THE HEXA PARALLEL ROBOT

In this section the Hexa parallel robot is detailed and the parameter optimization technique is applied on it in order to obtain the base angular layout, *i.e.* the position of the pairs of legs, which maximizes the angular displacement that can be applied to the end effector before entering into an unsafe zone with respect to direct singularity at a fixed position.

5.1 The Hexa parallel robot

The six DOF Hexa robot is composed by six limbs connecting the basis to the end effector, see Fig. 1. Each limb contains an active rotative joint A_i (for $i = 1, \cdots, 6$) fixed to the basis, a passive universal joint B_i (composed by two orthogonal rotative joints) and a passive spherical joint C_i connected to the end effector. The cranks and the passive links are connected at B_i.

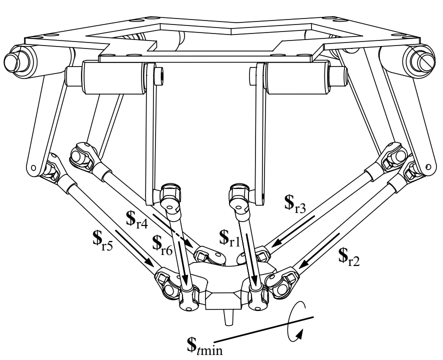

Figure 7. Hexa parallel robot: wrenches and end effector twist in Bier (2006)

The six limbs of the Hexa robot are arranged in three pairs of two active joints with collinear rotational axes, *i.e.* drive axes, see Fig. 7. The workspace is physically limited by a rotation constraint of the active rotative joints which avoid inverse kinematics singularities.

In this paper, the design parameters to be adjusted in order to improve the end effector angular rotation are the angular position of the pairs of leg in base, *i.e.* the base angular layout: α_1 and α_2, see Fig. 5 Therefore the problem may be stated as to find the optimum motor base angles (α_1 and α_2) aiming at obtaining the maximum safe end effector rotation θ around a given axis for a given end effector position (XYZ). The safe zone for end effector rotation is limited by the singularity index (δW_{lim}).

5.2 Numerical example

The application of the proposed procedure to a practical problem is detailed and discussed in the following paragraphs.

Let set the desired end effector position as $[-0.0100.010-0.450]$ (in meters) with respect to a coordinate system fixed to the central base point, and specify that the maximum desired rotation is about the $+Y$ axis θ_Y, *i.e.* from 0 degrees in positive direction. Thus, in the inner optimization, the singularity index $\delta W_{(min)}$ for each end effector location (in this case a fixed position and a changing orientation around Y) is calculated. At same time, in the outer optimization loop the maximum angle around Y (θ_Y), constrained to be into the safe zone, for the given position is found through inner point algorithm. The safe zone is limited by the singularity index value $\delta W_{lim} = 0.028$ as suggested by Hesselbach et al. (2005). Additionally, the constraints $\alpha_2 \geq \alpha_1 + 5°$, $\alpha_2 \leq 325°$ and $\alpha_1 \geq 50°$ are imposed, in order to bound the relation among the pairs of legs to feasible robot morphology. The objective function and constraint tolerances are both set up to 1e-6.

The complete optimization procedure is executed several times with random initial points and behaviors which systematically drives the constraint violation and first-order optimality criteria to acceptable values, as shown in Fig. 8.

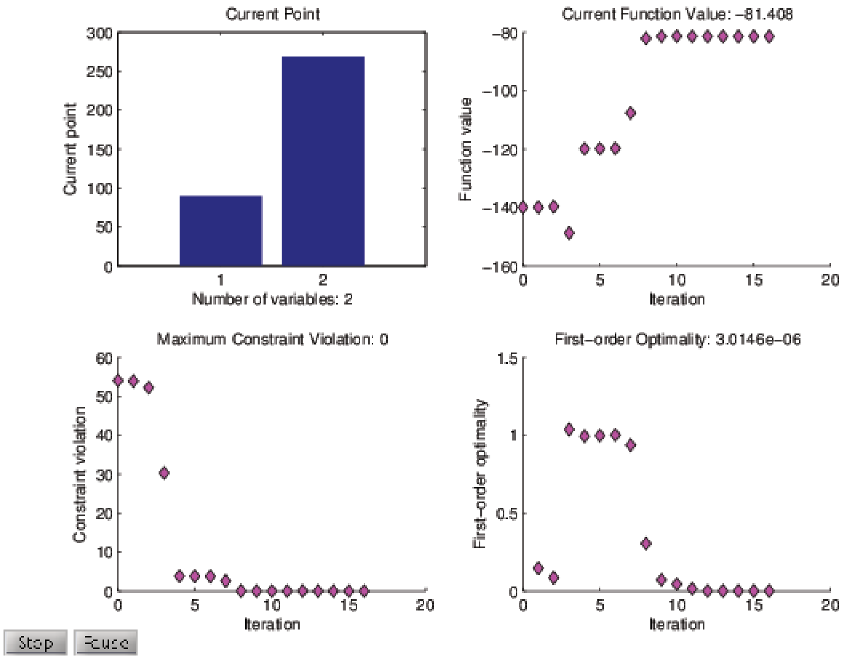

Figure 8. Graphical output from Matlab optimization process

However, three different optimum parameter sets (α_1, α_2) are obtained: $(90°, 269.1188°)$, $(172.7580°, 282.4482°)$ and $(90°, 175.6966°)$ whose respective angle D are $81.40°$, $88.28°$ and $87.29°$. Therefore, it may be concluded that this function possesses three optima, the best of them corresponding to $\alpha_1 = 172.7580°$ and $\alpha_2 = 282.4482°$, which allows a maximum twist ($88.28°$) around Y axis in the safe zone.

6. CONCLUSION

In this paper an optimization procedure to maximize the robot workspace based on a singularity index is presented. Considering that, for parallel robots, rotations are the most constrained motions, the selected end effector task to be optimized is an angular displacement.

Applying a two nested loop optimization, the layout angular position for the pairs of motors of the Hexa parallel robot is optimized. Therefore, using this layout, the robot reaches the maximum end effector rotation, for a given position, remaining out of singular zone. It is important to notice that three local optima which shown where found should be compared in order to establish the best one.

It is important to remark that setting the optimization problem in a mathematical programming framework provides flexibility to extend the procedure to deal with further complexities (more constraints or design variables, for instance) in a straightforward manner. This property will be explored in future works.

7. ACKNOWLEDGEMENTS

This work is being developed within the framework of the Research Project No. 7481/2010 "Parallel Robot Optimized Sinthesys for a Predefined Workspace" from CCT/UDESC.

8. REFERENCES

R. S. Ball. *A Treatise on the Theory of Screws*. Cambridge University Press, Cambridge, 1900. ISBN 0521636507 -re-printedg 1998.

Carlos Bier. *Geometrische und physikalische Analyse von Singularitäten bei Parallelstrukturen*. Vulkan-verlag, essen, Technische Universität Braunschweig, 2006.

A. Campos, C. Budde, and J. Hesselbach. A type synthesis method for hybrid robot structures. *Mechanism and Machine Theory*, 43(8), 2008.

A. Campos, R. Guenther, and D. Martins. Differential kinematics of parallel manipulators using assur virtual chains. *Proc. IMechE C, Journal of Mechanical Engineering Science*, 2223(7):1697–1711, 2009.

M. Ceccarelli. Screw axis defined by giulio mozzi in 1763 and early studies on helicoidal motion. *Mechanism and Machine Theory*, 35(6):761–770, June 2000.

M. Ceccarelli and C. Lanni. A multi-objective optimum design of general 3r manipulators for prescribed workspace limits. *Mechanism and Machine Theory*, 39(2):119–132, 2004. ISSN 0094114X. doi: 10.1016/S0094-114X(03)00109-5. cited By (since 1996) 25.

J. K. Davidson and K. H Hunt. *Robots and Screw Theory*. Oxford University Press, 2004.

Z. Gao, D. Zhang, and Y. Ge. Design optimization of a spatial six degree-of-freedom parallel manipulator based on artificial intelligence approaches. *Robotics and Computer-Integrated Manufacturing*, 26(2):180 – 189, 2010. ISSN 0736-5845. doi: DOI: 10.1016/j.rcim.2009.07.002.

Raphael Haftka and Zafer Gürdal. *Elements of structural optimization*. Kluwer Academic Publisher, 1991.

J. Hesselbach, A. Campos, C. Bier, and H. Löwe. Direct kinematic singularity detection of a hexa parallel robot. ICRA2005, IEEE, 2005.

K. Hunt. Dont't cross-thread the screw. In Hugh Hunt, editor, *Ball 2000 Conference*, pages 1–37, Trinity College, july 2000. University of Cambridge, Cambridge University Press.

K. H. Hunt. *Kinematic Geometry of Mechanisms*. Clarendon Press, Oxford, 1978.

B. Mayer and C. Gosselin. Singularity analysis and representation of the general gough-stewart platform. *International Journal of Robotics Research*, 19(3):271–288, march 2000.

J.P. Merlet. *Parallel Robots*. Kluwer Academic Publisher, 2000.

H. R. Mohammadi-Daniali, P. J. Zsombor-Murray, and J. Angeles. The kinematics of spatial double-traingular parallel manipulators. *Trans. ASME, Journal of Mechanical Design*, 117:658–661, December 1995.

L. Poinsot. Sur la composition des moments et la composition des aires. *J. Éc Polyt. Paris*, 6:182–205, 1806.

H. Pottmann, M. Peternell, and B. Ravani. Approximation in line space—applications in robot kinematics and surface reconstruction. In *Advances in robot kinematics: analysis and control (Salzburg, 1998)*, pages 403–412. Kluwer Acad. Publ., 1998a.

H. Pottmann, M. Peternell, and B. Ravani. Approximation in line space: applications in robot kinematics and surface reconstruction. In J. Lenarcic and M. L. Husty, editors, *Advances in Robot Kinematics: Analysis and Control*, pages 403–412. Kluwer Academic Publishers, 1998b.

S. Rao. *Optimization: Theory and Applications*. John Wiley and Sons Ltd ., 1978.

R.K. Rout, B.K.and Mittal. Parametric design optimization of 2-dof r-r planar manipulator-a design of experiment approach. *Robotics and Computer-Integrated Manufacturing*, 24(2):239–248, 2008. ISSN 07365845. doi: 10.1016/j.rcim.2006.10.008. cited By (since 1996) 12.

L. Sciavicco and B. Siciliano. *Modeling and Control of Robot Manipulators*. Electrical and Computer Engineering. McGraw-Hill, 1996. ISBN 0070572178.

M. Stock and K. Miller. Optimal kinematic design of spatial parallel manipulators: Application to linear delta robot. *Journal of Mechanical Design, Transactions of the ASME*, 125(2):292–301, 2003. ISSN 10500472. doi: 10.1115/1.1563632. cited By (since 1996) 47.

L. Tsai. *Robot Analysis: the Mechanics of serial and parallel manipulators*. John Wiley & Sons, New York, 1999. ISBN

0-471-32593-7.

G. Vanderplaats. *Numerical Optimization Techniques for Engineering Design: With Applications*. McGraw-Hill College, 1984.

P. Voglewede. *Measuring Closeness to Singularities of Parallel Manipulators with Application to the Design of Redundant Actuation*. PhD thesis, George W. Woodruff School of Mechanical Engineering, Georgia Institute of Technology, 2004.

P. Voglewede and I. Ebert-Uphoff. Measuring closeness to singularities for parallel manipulators. In *Proceedings - ICRA*, New Orleans, April 2004.

A. Wolf and M. Shoham. Investigation of parallel manipulators using linear complex approximation. *ASME, Journal of Mechanical Design*, 125(3):564–572, 2003.

Y. X. Xu, D. Kohli, and T. C. Weng. Direct differential kinematics of hybrid-chain manipulators including singularity and stability analyses. *Journal of Mechanical Design*, 116(2):614–621, June 1994.

A.a Yu, I.A.b Bonev, and P.a Zsombor-Murray. Geometric approach to the accuracy analysis of a class of 3-dof planar parallel robots. *Mechanism and Machine Theory*, 43(3):364–375, 2008. ISSN 0094114X. doi: 10.1016/j.mechmachtheory.2007.03.002. URL `http://www.scopus.com`. cited By (since 1996) 11.

D. Zhang, L. Wang, and E. Esmailzadeh. Pkm capabilities and applications exploration in a collaborative virtual environment. *Robotics and Computer-Integrated Manufacturing*, 22(4):384–395, 2006. ISSN 07365845. doi: 10.1016/j.rcim.2005.07.007. cited By (since 1996) 6.

J. Zhao, S. Zhang, J. Dong, Z. Feng, and K. Zhou. Optimizing the kinematic chains for a spatial parallel manipulator via searching the desired dexterous workspace. *Robotics and Computer-Integrated Manufacturing*, 23(1):38–46, 2007. ISSN 07365845. doi: 10.1016/j.rcim.2005.09.003. cited By (since 1996) 8.